Ligand Binding to Heme Proteins. V. Light-Induced Relaxation in Proximal Mutants L89I and H97F of Carbonmonoxymyoglobin

Yavuz Abadan,[§] Ellen Y. T. Chien,[*] Kelvin Chu,[§] Chester D. Eng,[§] G. Ulrich Nienhaus,[§] and Stephen G. Sligar[*‡]

Departments of [*]Biochemistry, [‡]Chemistry, and [§]Physics, University of Illinois at Urbana-Champaign, Urbana, Illinois 61801 USA

ABSTRACT We have studied the proximal mutants L89I and H97F of MbCO with FTIR and temperature-derivative spectroscopy at temperatures between 10 and 160 K. The mutations give rise only to minor alterations of the stretch spectra of the bound and photodissociated CO ligand. The most pronounced difference is a larger population in the A_3 substate at $\approx$1930 cm^{-1} in the mutants. The barrier distributions, as determined by temperature-derivative spectroscopy, are very similar to native MbCO after short illumination. Extended illumination leads to substantial increases of the rebinding barriers in native MbCO and the proximal mutants. A larger fraction of light-relaxed states is found in the proximal mutants, implying that the conformational energy landscape has been modified to more easily allow light-induced transitions. These and other spectroscopic data imply that the large changes in the binding properties are brought about by a light-induced conformational relaxation involving the structure at the heme iron. Similarities with spectral hole-burning studies and physical models are discussed.

INTRODUCTION

The binding of small ligands to heme proteins is probably one of the simplest biological processes, but it exhibits a stunning complexity when investigated in detail, for instance, in flash photolysis experiments on sperm whale MbCO over a wide range of time and temperature (Austin et al., 1975; Steinbach et al., 1991). Conceptually, the ligand-binding reaction can be divided into two steps, the access of the ligand to the active site and the bond formation step at the heme iron, so that the simplest kinetic scheme contains three wells along the reaction coordinate,

$$A \rightleftharpoons B \rightleftharpoons S.$$

Here A denotes the state where the ligand is bound to the heme iron, B is the state with the ligand in the heme pocket, and S is the state where the ligand is in the solvent.

Below $\approx$160 K, conformational motions are largely arrested, and the ligand cannot leave the protein. After photodissociation of MbCO with a short flash, rebinding from B to A is nonexponential and can be described with a temperature-independent distribution of activation enthalpies, $g(H)$, reflecting an inhomogeneous distribution of conformational substates (CS) with slightly different structures.

Above 160 K, conformational motions on the time scale of the ligand-binding process are thermally activated. Immediately after ligand dissociation, the protein still has a structure close to the bound state (Mb*), from which it subsequently relaxes to the equilibrium deoxy Mb structure (Agmon and Hopfield, 1983; Steinbach et al., 1991). The structural relaxation involves a substantial increase of the effective rebinding barrier, H, at the heme iron. Consequently, geminate rebinding slows, and the CO ligands can escape efficiently from the heme pocket through pathways created by protein fluctuations.

Evidence for the presence of the Mb* $\rightarrow$ Mb relaxation has been obtained through the shift of spectral lines and from the temperature and time dependence of the rebinding reaction (Friedman, 1985; Steinbach et al., 1991; Lambright et al., 1991; Nienhaus et al., 1992; Ansari et al, 1994; Jackson et al., 1994). Two spectroscopic markers indicate that the conformational relaxation involves changes in the stereochemistry of the heme iron: the relaxation is accompanied by shifts of band III, a charge transfer transition in the near-IR at $\approx$760 nm that is sensitive to the structure at the heme iron (Nienhaus et al., 1992; Jackson et al., 1994). The iron-H93 stretch band near 220 cm^{-1} shifts to lower wavenumbers upon relaxation (Friedman, 1985).

In hemoglobin and myoglobin, the heme iron is coordinated to the four pyrrole nitrogens of the porphyrin and the N_ϵ of the imidazole side chain of the proximal histidine, H93. It is believed that the protein structure on the proximal side of the heme can influence strongly the reactivity of the heme iron toward ligands. An extended network of hydrogen bonds and electrostatic interactions stabilizes the proximal side: the imidazole side chain of H93 is held in place by a bifurcated hydrogen bond from the N_δ-H to the backbone carbonyl oxygen of L89 and the O_γ of S92. The heme-7-propionic acid group forms hydrogen bonds with the N_ϵ of H97 and the O_γ of S92 (Cheng et al., 1991). As a result of these interactions, the imidazole plane is positioned in such a way that it comes close to eclipsing a line that connects the pyrrole nitrogens N_1 and N_3. This configuration is sterically unfavorable because of the close distances between the pyrrole nitrogens and the C_δ and C_ϵ protons of the imidazole ring. However, iterative Hückel theory calculations indicate that the eclipsed configuration is favored for electronic reasons because of

Received for publication 21 September 1994 and in final form 30 December 1994.

Address reprint requests to Dr. G. U. Nienhaus, Department of Physics, University of Illinois at Urbana-Champaign, 1110 West Green Street, Urbana, IL 61801-3080. Tel.: 217-333-6473; Fax: 217-333-9819; E-mail: uli@uiuc.edu.

0006-3495/95/06/2497/08 $2.00

interactions between metal $p\pi$ and imidazole $p\pi$ orbitals (Scheidt and Chipman, 1986). The structural details of how the proximal side influences the reactivity at the heme iron are not yet clear.

Site-directed mutagenesis is a powerful tool for investigating the structure-function relation. A large number of mutant studies aiming at elucidation of the functional importance of key residues on the distal side of the heme group have been published (Nagai et al., 1987; Braunstein et al., 1988; Olson et al., 1988; Springer et al., 1989; Mathews et al., 1989; Egeberg et al., 1990a; Carver et al., 1991; Lambright et al., 1994). Although proximal mutants have been around for quite a long time (Egeberg et al., 1990b; Adachi et al., 1993), detailed structural and functional studies have been reported only recently (Smerdon et al., 1993; Barrick, 1994; DePillis et al., 1994). A particularly elegant approach is the one chosen by Barrick (1994), where the proximal histidine is replaced by a glycine so that an internal cavity is created in which free imidazole and other proximal ligands can bind to the heme iron.

To examine the influence of the proximal side on the ligand-binding properties, we have used site-directed mutagenesis to modify conserved residues on the proximal side that are involved in the proximal hydrogen bond network. The leucine at position 89 was replaced by an isoleucine (L89I), and the histidine at position 97 was replaced by a phenylalanine (H97F). Here we report spectroscopic and kinetic properties of the CO-liganded mutants using Fourier transform infrared spectroscopy (FTIR) and temperature-derivative spectroscopy (TDS) in the IR stretch bands of the CO ligand.

MATERIALS AND METHODS

Sample preparation

Mutations of sperm whale myoglobin at positions 89 and 97 were generated using site-directed mutagenesis following procedures described by Springer et al. (1989). Oligonucleotides were synthesized by the University of Illinois Biotechnology Center and purified by reverse-phase HPLC as described by Springer and Sligar (1987). Mutant sequences were confirmed using the Sequenase double-stranded DNA sequencing reagents and protocol from United States Biochemicals (Cleveland, OH). Mutant sperm whale myoglobin were expressed in *Escherichia coli* using the synthetic gene of Springer and Sligar (1987) with the amino acid at position 122 corrected to aspartic acid (Phillips et al., 1990). DNA manipulations were essentially as described by Sambrook et al. (1989), using reagents from New England Biolabs (Beverly, MA) or Gibco-Bethesda Research Labs (Grand Island, NY). Radiochemicals were purchased from Amersham (Arlington Heights, IL). Unless otherwise noted, all other reagents were purchased from Sigma Chemical Co. (St. Louis, MO).

The proteins were purified essentially as described by Springer and Sligar (1987) with the following modifications. The pH of the cell lysate was adjusted to 5.9 with NaH_2PO_4. The solution was stirred for 30 min at 4°C, and precipitates were removed by centrifugation at 30,000 rpm for 30 min. The protein solution was diluted fourfold with water and then loaded on a CM-52 cellulose cation exchange column (Whatman, Hillsboro, OH) equilibrated with 10 mM Na_2PO_4, pH 6.0, and eluted with a linear pH gradient: 10 mM Na_2PO_4, pH 6.0, to 30 mM Na_2HPO_4. This procedure resulted in a homogeneous solution of Mb as monitored by SDS-PAGE.

For the experiments, freeze-dried myoglobin powder was dissolved in a mixture of 75% glycerol and 25% 0.4 M phosphate buffer solution (v/v). The solution was reduced with $Na_2S_2O_4$ to give deoxy Mb. MbCO was obtained by stirring for several hours under a CO atmosphere. The protein concentration of the samples was ≈15 mM.

FTIR/TDS

The ligand-binding properties were investigated using FTIR spectroscopy. Transmittance spectra were collected on a Sirius 100 FTIR spectrometer (Mattson, Madison, WI) between 1800 and 2200 cm^{-1} with a resolution of 2 cm^{-1}. The protein samples were kept between two sapphire windows separated by a 75-μm-thick mylar washer inside a block of oxygen-free, high conductivity copper that was mounted on the cold-finger of a closed-cycle helium refrigerator (CTI Cryogenics, model 22 C, Waltham, MA). The temperature was measured with a silicon temperature sensor diode and regulated with a digital temperature controller (Lake Shore Cryotronics, model DRC93C, Westerville, OH). The MbCO sample was photolyzed with light from an argon ion laser (Omnichrome, model 543, Chino, CA). The laser was operated at 300-mW multimode output and emitted predominantly at 488 and 514 nm. The beam was split and focused with lenses on the sample from both sides. The photolysis rate coefficient, k_L, was determined as ≈20 s^{-1} at low temperatures.

To assess the rebinding barriers, TDS was used. TDS is a protocol designed to measure thermally activated rate processes with distributed barriers (Berendzen and Braunstein, 1990). The measurement is started with a completely photodissociated sample at 12 K, where rebinding is extremely slow on the experimental time scale. Subsequently, while ramping the sample temperature T_R linearly up in time, FTIR transmittance spectra are taken continuously. FTIR absorbance difference spectra are then calculated from spectra at successive temperatures:

$$\Delta\mathscr{A}(\nu, T_R) = \log \mathscr{T}(\nu, T_R - K) - \log \mathscr{T}(\nu, T_R + \tfrac{1}{2} K).$$

The change in spectral area, $\Delta\mathscr{A}(\nu, T_R)$, is proportional to the population, ΔN, that rebinds at temperature T_R. The TDS signal, $\Delta\mathscr{A}(\nu, T_R)$, approximates the distribution of enthalpy barriers for rebinding, $g(H)$. Given a first-order reaction and the Arrhenius relation, the temperature T_R can be converted into an activation enthalpy H (in this paper, we use the preexponential $A = 8 \times 10^8$ s^{-1} for the A_1 substate of MbCO (Steinbach et al., 1991)). The relation between T_R and H is linear to a good approximation, so the temperature axis can be treated as an enthalpy axis. Details of the method are given by Berendzen and Braunstein (1990).

The effect of extended illumination on the barrier distribution was studied by exposing the samples to light from the Ar ion laser before the TDS measurement. While illuminating, the sample was cooled from 160 to 12 K at a rate of 12 K/h. Experimental details of this protocol have been reported in a recent paper (Nienhaus et al., 1994).

RESULTS

Infrared difference spectra of native myoglobin and the L89I and H97F mutants at 12 K (light − dark) are shown in Fig. 1. The IR spectra of the heme-bound CO around 1950 cm^{-1} are similar, showing the three A substates, A_0 (≈1966 cm^{-1}), A_1 (≈1945 cm^{-1}), and A_3 (≈1930 cm^{-1}). Table 1 summarizes parameters from least-squares fits of Voigtian lines to the spectra. The A substates have been explained by different conformations of the imidazole side chain of the distal histidine, H64, which gives rise to different electrostatic interactions that affect the CO bond order (Maxwell and Caughey, 1976; Park et al., 1991; Ray et al., 1993). The wavenumbers of the three A states in the mutants are only slightly shifted from those of the native MbCO sample. Most pronounced is the red shift of the A_1 substate of the H97F mutant. The populations in the A substates differ for the three samples,

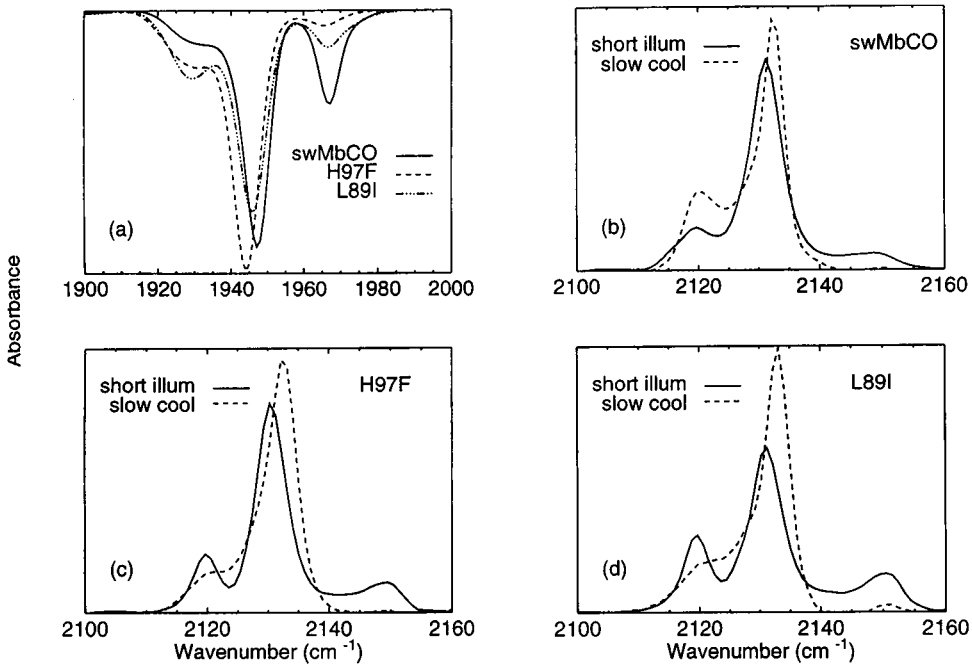

FIGURE 1 FTIR difference spectra of native myoglobin and proximal mutants showing the *A* substates (heme-bound CO) between 1900 and 2000 cm^{-1} and the *B* substates (photodissociated CO in the heme pocket) between 2100 and 2160 cm^{-1}.

and A_3 in the proximal mutants is significantly more populated than in native MbCO. Obviously, the structural modifications on the proximal side affect the CO binding on the distal side, although in a subtle way.

B substate spectra are shown in Fig. 1 *b-d* (*solid lines*). For native MbCO, the connections between the *A* and *B* substates have been reported recently (Mourant et al., 1993). There is no one-to-one mapping between *A* and *B* substates, but a single *A* substate can be photodissociated into several *B* substates. The proximal mutants show similar *B* substates as the native samples, indicating only minor structural alterations with respect to the ligand-binding positions in the heme pocket.

Ligand-binding properties at cryogenic temperatures were examined using temperature-derivative spectroscopy. Fig. 2 *a* shows a TDS contour map of native MbCO (pH 6.8) that was obtained after illumination of the sample for 5 s. Three peaks appear, corresponding to rebinding to the three *A* substates. The peak of A_0 is at a slightly lower temperature than the one of A_1, whereas A_3 rebinds at a markedly higher temperature. These observations are consistent with the results of low temperature flash photolysis experiments with monitoring in the individual *A* substates (Steinbach et al., 1991; Young et al., 1991). Very similar results were obtained for the L89I and H97F mutants, as seen in Fig. 3 *a*, where we show cuts through the contour maps along the temperature axis for the A_1 substates of the three myoglobins studied.

TABLE 1 Spectroscopic data of native and mutant A states

System	*A* state	Population (%)	ν_{pk} (cm^{-1})	Γ (cm^{-1})
Native, pH 6.8	A_0	13.5	1966.6	7.7
	A_1	70.9	1946.3	9.0
	A_3	15.6	1930.8	12.6
L89I, pH 7.0	A_0	10.0	1967.4	10.5
	A_1	65.3	1945.7	9.5
	A_3	24.7	1929.4	13.7
H97F, pH 6.8	A_0	3.2	1966.1	8.6
	A_1	74.2	1944.2	8.8
	A_3	22.6	1929.2	15.8

Peak positions ν_{pk} and widths Γ (full width at half-maximum) were obtained from least-squares fits of a sum of Voigtians to the data. Errors on peaks and widths are ± 0.5 cm^{-1}.

Extended illumination of MbCO at cryogenic temperatures slows ligand rebinding (Chance et al., 1986; Ansari et al., 1987; Powers et al., 1987; Srajer et al., 1991; Ahmed et al., 1991). Substantial changes of the low temperature barrier distributions with enormous increases of the rebinding enthalpies have been observed (Nienhaus et al., 1994). The changes are not permanent; after complete recombination, the normal barrier distribution is recovered. The effect has been interpreted as light-induced structural relaxations of the protein. We have shown that the heights of the barriers that are generated by illumination are sensitive to the temperature at which the sample is illuminated: the higher the illumination temperature, the higher are the barriers of the light-relaxed states. To get an overall view of the light-induced changes, the sample is illuminated with an argon ion laser while the temperature is decreased linearly in time from 160 to 12 K over a period of several hours. At high temperature, high barrier states are generated. By decreasing the temperature, recombination rates of these molecules are reduced and rebinding is prevented. At lower temperature, molecules with lower barriers are generated and, by slowly cooling the sample, light-relaxed states are created over the entire temperature range. At 12 K, the light is switched off and the TDS measurement is started to assess the rebinding barrier distributions.

We have studied the light-induced relaxation in native myoglobin and in the proximal mutants after slow cooling

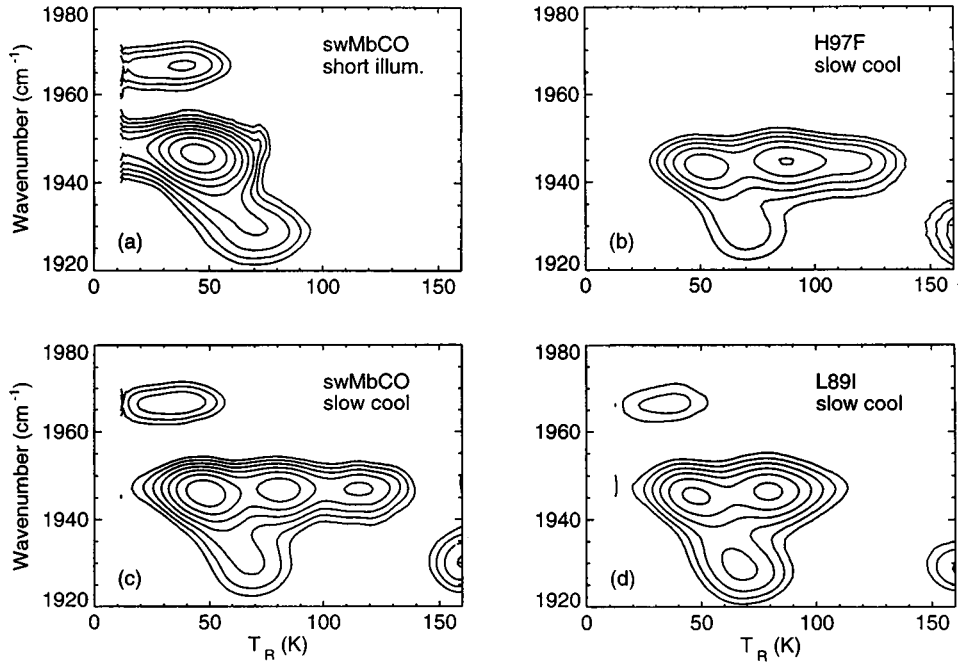

FIGURE 2 TDS contour maps of the *A* substate region of swMbCO and the proximal mutants. (*a*) TDS map after complete photolysis (k_L = 5 s^{-1}, t_L = 5 s). (*b* and *c*) TDS map after cooling under illumination from 160 to 10 K at a rate of 10 K/h.

under light. Fig. 2 *b-d* shows the resultant barrier distributions for the three samples as contour plots. At temperatures below ≈160 K, interconversions between the *A* substates are arrested (Young et al., 1991) so that the relative populations of the *A* substates do not change upon illumination. However, within each *A* substate, a large fraction of molecules acquire barriers that are much higher than those seen after a short, photolyzing flash. The A_1 distributions that are obtained after slow cooling under illumination are substantially different for the three samples (Fig. 3 *b*). The TDS data can be fitted well with a sum of Gaussian enthalpy distributions. In Table 2, the peak enthalpies of these distributions are listed. For the short illumination data (Fig. 3 *a*), one Gaussian is sufficient, with $H_{pk_{B^0}} \approx 10$ kJ/mol. Previously, we have shown that extended illumination in native MbCO leads to discrete light-relaxed populations, which we labeled with B^1, B^2, and B^3. B^1 is close to the normal distribution and is difficult to separate. For the slow-cool data (Fig. 3 *b*), a sum of three Gaussian enthalpy distributions is necessary, with positions, $H_{pk_{B^0/B^1}}$, $H_{pk_{B^2}}$, and $H_{pk_{B^3}}$. For native MbCO, most of the population stays near 45 K (≈10 kJ/mol), close to the normal barrier distribution seen after a short, photolyzing flash. Two additional peaks occur at 80 K (≈18.5 kJ/mol) and 125 K (≈27 kJ/mol). For the H97F mutant, there are also three peaks. In this sample, however, the majority of the population is found in a large peak at 90 K (≈20 kJ/mol). The L89I mutant also shows a strong second peak, but only a small population at higher enthalpies. For a good fit, a 5% population at ≈24 kJ/mol has to be included. The A_3 substate does not show relaxed populations below 150 K in any of the three samples, but a substantial fraction is observed in a peak near 160 K.

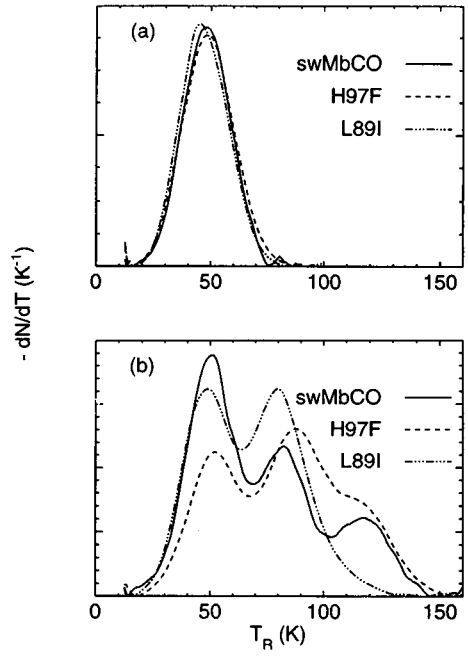

FIGURE 3 Absorbance difference, $\Delta A(T_R)$, integrated between 1945 and 1950 cm^{-1}: (*a*) after short illumination (25 photons/molecule), or (*b*) slow cooling from 160 to 10 K at a rate of 10 K/h.

To study the light-induced relaxation in the A_0 substate, we performed experiments with samples at lower pH, where A_0 is more populated. Contour maps of the data are shown in Fig. 4. Although the light-induced relaxation in A_0 of native MbCO shows two weakly populated peaks at 95 and 130 K, H97F has a very strong peak at 70 K upon illumination. A mapping between the wavenumber and the population of the peaks is also evident. The peak at 70 K is preferentially populated by molecules on the blue side of the A_0 band.

TABLE 2 Peak enthalpies of the A_1 substate

System	pH	$H_{pk_B^0}$ (kJ/mol)	$H_{pk_{B^0B^1}}$ (kJ/mol)	$H_{pk_B^2}$ (kJ/mol)	$H_{pk_B^3}$ (kJ/mol)
Native	6.8	10.2	10.6	18.5	27.0
L89I	7.0	10.1	10.4	18.1	24.3
H97F	6.8	10.5	11.4	19.7	27.0

The Gaussian distributions of rebinding enthalpies are characterized by peak enthalpies H_{pk}, using preexponentials determined from flash-photolysis measurements on native swMbCO (Steinbach et al., 1991). $H_{pk_B^0}$ denotes the peak of the barrier distribution after short illumination (Fig. 3 *a*), the other three H_{pk} values refer to the slow-cool barrier distributions (Fig. 3 *b*). Errors on enthalpies are ±0.5 kJ/mol.

In Fig. 1 *b-d*, the *B* substate spectra after a short pulse at 12 K (*solid lines*) are compared with those obtained after slow cooling from 160 to 12 K (*dashed lines*). The main difference is that the absorption above 2140 cm^{-1} is practically depleted in all three samples when cooling under illumination, and additional population appears at 2133 cm^{-1}. These changes imply a transition from ≈2150 cm^{-1} to ≈2133 cm^{-1}. Transitions between *B* substates at low temperatures have been observed earlier in the exchange between *B*2119 and *B*2131/*B*2149 at temperatures ≈20 K and are interpreted as motions of the CO in the heme pocket (Alben et al., 1982; Mourant et al., 1993). The transitions can be explained with a simple model: assume that the free energy of *B*2150 is higher than that of *B*2133. When photolyzing at 12 K, the barrier between the states may be too high to overcome, and part of the population remains stuck in *B*2150. However, upon cooling under illumination, molecules are photodissociated at a temperature sufficiently high to overcome the barrier and relax into the the state *B*2133 with lower free energy. The connection between the *B*2133 and *B*2150 substates is in agreement with the mapping by Mourant et al. (1993), where both peaks were assigned to the A_3 substate.

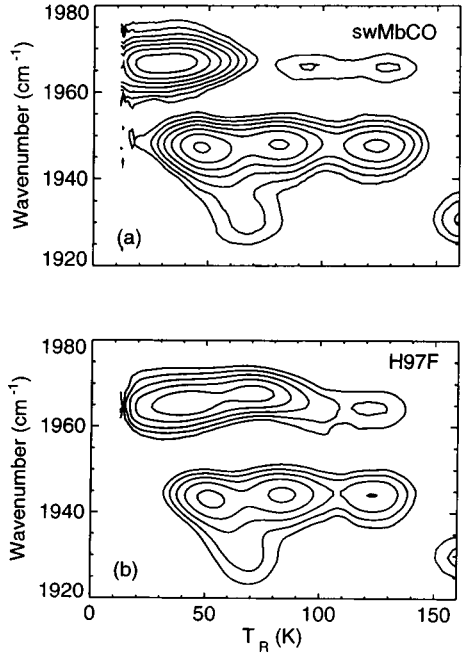

FIGURE 4 TDS contour maps of the *A* substate region of (*a*) native swMbCO at pH 5.7 and (*b*) the H97F mutant at pH 5.7.

DISCUSSION AND CONCLUSIONS

After short illumination, the proximal mutants H97F and L89I have barrier distributions for CO rebinding that are not much different from those of the native protein. By contrast, in the distal pocket mutant H64, substantially lower activation enthalpy barriers were observed, with a peak enthalpy of ≈6 instead of ≈10 kJ/mol for the native protein (Braunstein et al., 1988).

Surprising increases in the barrier heights can be induced by extended illumination (Table 2), much larger than the changes in the distal pocket mutant, and the barrier distributions obtained by cooling under light are markedly different for the three samples studied. The present study gives only information about the kinetic properties of the states that are created by extended illumination. Two spectroscopic markers, band III and the Fe-His Raman line, indicate that the drastic increase of the rebinding barriers is effected by transitions involving the structure around the heme iron.

The near-infrared band III (≈760 nm) is at a higher wavenumber in deoxy Mb than in photodissociated MbCO at 4.2 K, and Iizuka et al. (1974) therefore called it the "conformation band." It has been assigned to a porphyrin-to-iron charge transfer transition $a_{2u} \rightarrow d_{yz}$ (Eaton and Hofrichter, 1981). The band is inhomogeneously broadened and shows an approximately linear mapping between the wavenumber and the rebinding enthalpy of a homogeneous subpopulation in MbCO (and other heme proteins), so that molecules on the red side of the band have low barriers and those on the blue side have high barriers (Campbell et al., 1987; Steinbach et al., 1991). All of these properties reflect the sensitivity of band III to the local structure at the heme iron. We have shown recently that the light-induced relaxation in MbCO is accompanied by a shift of band III toward the deoxy Mb position (Nienhaus et al., 1994). However, the major part of the shift occurs above 160 K (Nienhaus et al., 1992), where large scale motions are thermally activated. This general behavior was also observed for the H97F and L89I mutants (data not shown).

Resonance Raman studies of the Fe-H93 stretch band ($\nu_{Fe—His} \approx 220$ cm^{-1}) provide more structural information of the vicinity of the heme iron (Nagai et al., 1980; Friedman, 1985; Champion, 1988; Kitagawa, 1988; Rousseau and Friedman, 1988; Gilch et al., 1993). The band is sensitive to structural changes that affect the ligand-binding properties. In general, $\nu_{Fe—His}$ shifts to lower wavenumbers when hemoglobin switches from the R to the T conformation.

Friedman and collaborators measured the temperature dependence of ν_{Fe-His} in photodissociated MbCO (Ahmed et al., 1991). Upon extended illumination, they noticed large changes in the area of the line with respect to heme modes, whereas the frequency remained constant in the temperature range discussed here. For temperatures above ≈160 K, pronounced frequency shifts were observed. Friedman et al. (1990) suggested a model that connects the area and frequency of this Raman line to the two angles that specify the position of the proximal histidine (H93) imidazole side chain to the heme, the tilt angle θ of the Fe-H93 with respect to the heme normal and the azimuthal angle ϕ that measures the rotation of the imidazole plane away from the line connecting pyrrole nitrogens N_1 and N_3. Within this model, an increase in the tilt angle θ leads to a decrease of the frequency and an increase of the intensity. An increase in ϕ leads to an decrease in intensity, leaving the frequency unchanged. The marked increase in the area of ν_{Fe-His} upon extended illumination (Ahmed et al., 1991) thus is explained by a rotation of the imidazole side chain around the iron-histidine bond toward smaller ϕ angles. The fact that the frequency of ν_{Fe-His} in MbCO does not shift upon extended illumination at cryogenic temperatures implies that, although the barriers increase substantially, the tilt angle remains constant. Changing the tilt angle involves large scale motions, in particular, a shift of the F helix. Such motions are arrested at temperatures below the glass transition of the solvent. Most likely, the shift of band III above 160 K indicates the onset of large-scale motions (Nienhaus et al., 1992).

The response of spectroscopic observables to extended illumination indicates alterations in the environment of the heme iron, either from motions of the heme group or from changes in the linkage of the heme iron to the polypeptide chain. This raises the question: What is the mechanism by which photon absorption leads to conformational relaxation? A physical model of the process should explain the following characteristics. 1) *The relaxation is photon-induced.* After photodissociation, the protein is in a nonequilibrium photoproduct structure (Mb*), and scenarios have been suggested where the relaxation occurs thermally in the dark at temperatures where recombination is negligible (Ansari et al., 1987). We have kept MbCO samples in the dark for many hours at low temperatures without observing any changes of the barrier distribution. Therefore, it is clear that photon absorption is essential for the structural changes to occur. 2) *The efficacy of creating light-relaxed states does not depend on whether the CO ligand is bound or not.* When illuminating at temperature T_L, proteins with enthalpy barrier $H_{BA} < RT_L$ predominantly absorb photons while they are in the ligated state, whereas the population with higher barriers is, on the average, photodissociated. If the effect were sensitive on the ligation state, we would have expected a discontinuity in the yield as a function of barrier H_{BA}, which was not observed (Nienhaus et al., 1994). 3) *The light-induced relaxations are not diffusive but occur in discrete steps.* The data in Fig. 3 *b* show well separated light-relaxed barrier distributions. They are markedly different for the mutants and native MbCO. Thus, transitions between these states are affected by the proximal modifications. 4) *The yield of generating light-relaxed states is distributed* (Nienhaus et al., 1994; Chu et al., 1995). Furthermore, the relaxed states are characterized by wide $g(H_{BA})$ distributions. 5) *After ligand recombination, a "normal" barrier distribution is observed after short illumination.* Consequently, light does not lead to permanent changes of the molecules.

Similarities exist between the light-induced relaxation and spectral hole burning of fluorescent dyes embedded in glassy matrices (Friedrich and Haarer, 1984; Shu and Small, 1992). Hole-burning experiments make use of the fact that electronic absorption bands of dye molecules in glasses are inhomogeneously broadened because of the heterogeneous local environment, whereas the homogeneous linewidth is very small, reflecting the long lifetime of the excited state. In nonphotochemical hole burning (NPHB), the dye molecules do not undergo chemical changes upon illumination. Nevertheless, excitation with a narrow-band laser leads to narrow holes in the inhomogeneous line because irradiation changes the conformation around a selected subset of chromophores so that they absorb at a different wavelength after the burn. The hole-burning yield (hole area/number of photons) changes dramatically upon deuteration, implying that hydrogen-bonded hydrogens are involved in the structural changes (Berg et al., 1988). The yields of hole burning and filling are distributed.

The motions that are observed in NPHB are not completely understood, but models normally involve two-level systems (TLS) due to bistable configurations of the dye in the glassy host matrix. In the model by Bogner and Schwarz (1981), hopping between the TLS states is induced by nonthermal photons localized at the dye probe that arise from the decay of the electronically excited state. Hayes and Small (1978) proposed a model where the barrier that separates the TLS states is much smaller in the excited state than in the ground state. Transitions occur by crossing of the barrier while the system is in the excited state. In an extension of this model (Shu and Small, 1992), an "outside-in hierarchy" of dynamic events was invoked where electronic excitation leads to a decrease of free volume in the host matrix, while the free volume of the dye itself increases, thus enabling the conformational transition. The dependence of the hole-burning spectra on burn temperature was explained by thermally assisted, photon-induced relaxation processes.

Proteins have glass-like properties (Iben et al., 1989) and, hence, it is not surprising that hole-burning studies can be done on chromophores embedded in proteins (Reddy et al., 1992; Zollfrank et al., 1992). There is, however, an important difference between hole burning and the experiments reported in this paper. The lifetime of the electronically excited state of the heme group is on the order of 100 fs and, hence, the time for barrier crossing in the electronically excited state, as suggested by Shu and Small (1992), is a factor 10^4 smaller than that of typical NPHB dyes. If we assume similar barrier-crossing rates, the yield of light-relaxed states should

be four orders of magnitude smaller. The yields of light-relaxed states in MbCO, however, are quite substantial (Chu et al., 1995). Similar to the dependence of NPHB on the burn temperature, our experiments reveal that the barrier distributions that are created by extended illumination are very sensitive to the average sample temperature (Nienhaus et al., 1994), which makes it unlikely that the transient increase of the chromophore temperature of several hundred kelvin after electronic relaxation (Henry et al., 1986; Li and Champion, 1994), according to the scenario of Bogner and Schwarz (1981), is important for the mechanism. Also, in the case that photodissociation follows the electronic excitation, much less energy is available for dissipation in the form of heat compared with absorption by an already dissociated molecule. However, the yield of light-relaxed states does not depend on the ligation state (Nienhaus et al., 1994). Another important difference between our experiments and hole burning is that our effects extend to higher temperatures. To summarize, a simple "local heating model" that leads to an annealing of the structure is insufficient to explain the phenomena accompanying these experiments.

Recently, the x-ray structures of the MbCO photoproduct at low temperatures have been determined (Schlichting et al., 1994). X-ray crystallography at cryogenic temperatures may be a useful tool to substantiate the conclusions drawn from the spectroscopic observations. One may hope that the light-induced changes of the structure that lead to the drastic changes of functional properties have sufficiently large amplitude so that they can be pinpointed. The fact that the light-relaxed populations can be populated much more easily in the proximal mutants makes them particularly attractive for the determination of the structure of relaxed intermediates.

We thank D. Ehrenstein, H. Frauenfelder, B. McMahon, J. Müller, and R. D. Young for their collaboration and helpful criticism, and S. G. Boxer for constructive remarks on the manuscript.

This work was supported by National Institutes of Health (grant GM 18051) and the Office of Naval Research (grant N00014–92-J-1942).

REFERENCES

Adachi, S., S. Nagano, K. Ishimori, Y. Watanabe, I. Morishima, T. Egawa, T. Kitagawa, and R. Makino. 1993. Roles of proximal ligand in heme proteins: replacement of proximal histidine of human myoglobin with cysteine and tyrosine by site-directed mutagenesis as models for P-450, chloroperoxidase, and catalase. *Biochemistry*. 32:241–252.

Agmon, N., and J. J. Hopfield. 1983. CO binding to heme proteins: a model for barrier height distributions and slow conformational changes. *J. Chem. Phys.* 79:2042–2053.

Ahmed, A. M., B. F. Campbell, D. Caruso, M. R. Chance, M. D. Chavez, S. H. Courtney, J. M. Friedman, I. E. T. Iben, M. R. Ondrias, and M. Yang. 1991. Evidence for proximal control of ligand specificity in hemeproteins: absorption and Raman studies of cryogenically trapped photoproducts of ligand bound myoglobins. *Chem. Phys.* 158:329–352.

Alben, J. O., D. Beece, S. F. Bowne, W. Doster, L. Eisenstein, H. Frauenfelder, D. Good, J. D. McDonald, M. C. Marden, P. P. Moh, L. Reinisch, A. H. Reynolds, E. Shyamsunder, and K. T. Yue. 1982. Infrared spectroscopy of photodissociated carboxymyoglobin at low temperatures. *Proc. Natl. Acad. Sci. USA*. 78:2903–2907.

Ansari, A., J. Berendzen, D. Braunstein, B. R. Cowen, H. Frauenfelder, M. K. Hong, I. E. T. Iben, J. B. Johnson, P. Ormos, T. B. Sauke, R. Scholl, A. Schulte, P. J. Steinbach, J. Vittitow, and R. D. Young. 1987. Rebinding and relaxation in the myoglobin pocket. *Biophys. Chem.* 26:337–355.

Ansari, A., C. M. Jones, E. R. Henry, J. Hofrichter, and W. A. Eaton. 1994. Conformational relaxation and ligand binding in myoglobin. *Biochemistry*. 33:5128–5145.

Austin, R. H., K. W. Beeson, L. Eisenstein, H. Frauenfelder, and I. C. Gunsalus. 1975. Dynamics of ligand binding to myoglobin. *Biochemistry*. 14:5355–5373.

Barrick, D. 1994. Replacement of the proximal ligand of sperm whale myoglobin with free imidazole in the mutant His-93 → Gly. *Biochemistry*. 33:6546–6554.

Berendzen, J., and D. Braunstein. 1990. Temperature-derivative spectroscopy: a tool for protein dynamics. *Proc. Natl. Acad. Sci. USA*. 87:1–5.

Bogner, U., and R. Schwarz. 1981. Laser-induced changes in the sideband shape of selectively excited dyes in noncrystalline organic solids at 1.3 K. *Phys. Rev. B*. 24:2846–2849.

Braunstein, D., A. Ansari, J. Berendzen, B. R. Cowen, K. D. Egeberg, H. Frauenfelder, M. K. Hong, P. Ormos, T. B. Sauke, R. Scholl, A. Schulte, S. G. Sligar, B. A. Springer, P. J. Steinbach, and R. D. Young. 1988. Ligand binding to synthetic mutant myoglobin (His-E7 → Gly): role of distal histidine. *Proc. Natl. Acad. Sci. USA*. 85:8497–8501.

Campbell, B. F., M. R. Chance, and J. R. Friedman. 1987. Linkage of functional and structural heterogeneity in proteins: dynamic hole burning in carboxymyoglobin. *Science*. 238:373–376.

Carver, T. E., J. S. Olson, S. J. Smerdon, S. Krzywda, A. J. Wilkinson, Q. H. Gibson, R. S. Blackmore, J. D. Ropp, and S. G. Sligar. 1991. Contributions of residue 45(CD3) and heme-6-propionate to the bimolecular and geminate recombination reactions of myoglobin. *Biochemistry*. 30: 4697–4705.

Champion, P. 1988. Cytochrome P450 and the transform analysis of heme protein Raman spectra. *In* Biological Applications of Raman Spectroscopy. T. G. Spiro, editor. John Wiley & Sons, New York. 249–292.

Chance, B., K. Korszun, S. Khalid, C. Alter, J. Sorge, and E. Gabbidon. 1986. Time-resolved studies of active site structural changes in solution. *In* Structural Biological Applications of X-Ray Absorption, Scattering, and Diffraction. H. D. Bartunik and B. Chance, editors. Academic Press, New York. 49–71.

Cheng, X., and B. P. Schoenborn. 1991. Neutron diffraction study of carbonmonoxymyoglobin. *J. Mol. Biol.* 220:381–399.

Chu, K., R. M. Ernst, H. Frauenfelder, J. R. Mourant, G. U. Nienhaus, and R. Philipp. 1995. Light-induced and thermal relaxation in a protein. *Phys. Rev. Lett.* 74:2607–2610.

DePillis, G. D., S. M. Decatur, D. Barrick, and S. G. Boxer. 1994. Functional cavities in proteins: a general method for proximal ligand substitution in myoglobin. *J. Am. Chem. Soc.* 116:6981–6982.

Eaton, W. A., and J. Hofrichter. 1981. Polarized absorption and linear dichroism spectroscopy of hemoglobin. *Methods Enzymol.* 76:175–261.

Egeberg, K. D., B. A. Springer, S. G. Sligar, T. E. Carver, R. J. Rohlfs, and J. S. Olson. 1990a. The role of Val^{98}(E11) in ligand binding to sperm whale myoglobin. *J. Biol. Chem.* 265:11788–11795.

Egeberg, K. D., B. A. Springer, S. A. Martinis, S. G. Sligar, D. Morikis, and P. M. Champion. 1990b. Alteration of sperm whale myoglobin heme axial ligation by site-directed mutagenesis. *Biochemistry*. 29:9783–9791.

Friedman, J. 1985. Structure, dynamics, and reactivity in hemoglobin. *Science*. 228:1273–1280.

Friedman, J., B. F. Campbell, and R. W. Noble. 1990. A possible new control mechanism suggested by resonance Raman spectra from a deep ocean fish hemoglobin. *Biophys. Chem.* 37:43–59.

Friedrich, J., and D. Haarer. 1984. Photochemical hole burning: a spectroscopic study of relaxation processes in polymers and glasses. *Angew. Chem. Int. Ed. Engl.* 23:113–140.

Gilch, H., R. Schweitzer-Stenner, and W. Dreybrodt. 1993. Structural heterogeneity of the Fe^{2+}-Nϵ(His^{F8}) bond in various hemoglobin and myoglobin derivatives probed by the Raman-active iron histidine stretching mode. *Biophys. J.* 65:1470–1485.

Hayes, J. M., and G. J. Small. 1978. Non-photochemical hole burning and impurity site selection in organic glasses. *Chem. Phys.* 27:151–157.

Henry, E. R., W. A. Eaton, and R. M. Hochstrasser. 1986. Molecular dynamics simulations of cooling in laser-excited heme proteins. *Proc. Natl. Acad. Sci. USA*. 83:8982–8986.

Iben, I. E. T., D. Braunstein, W. Doster, H. Frauenfelder, M. K. Hong, J. B. Johnson, S. Luck, P. Ormos, A. Schulte, P. J. Steinbach, A. H. Xie, and R. D. Young. 1989. Glassy behavior of a protein. *Phys. Rev. Lett.* 62:1916–1919.

Iizuka, T., H. Yamamoto, M. Kotani, and T. Yonetani. 1974. Low temperature photodissociation of heme proteins: carbon monoxide complex of myoglobin and hemoglobin. *Biochim. Biophys. Acta.* 371:1715–1729.

Jackson, T. A., M. Lim, and P. A. Anfinrud. 1994. Complex nonexponential relaxation in myoglobin after photodissociation of MbCO — measurement and analysis from 2 ps to 56 μs. *Chem. Phys.* 180:131–140.

Kitagawa, T. 1988. Heme protein structure and the iron histidine stretching mode. *In* Biological Applications of Raman Spectroscopy. T. G. Spiro, editor. John Wiley & Sons, New York. 97–132.

Lambright, D. G., S. Balasubramanian, and S. G. Boxer. 1991. Protein relaxation dynamics in human myoglobin. *Chem. Phys.* 158:249–260.

Lambright, D. G., S. Balasubramanian, S. M. Decatur, and S. G. Boxer. 1994. Anatomy and dynamics of a ligand-binding pathway in myoglobin: the roles of residues 45, 60, 64, and 68. *Biochemistry.* 33:5518–5525.

Li, P., and P. M. Champion. 1994. Investigations of the thermal response of laser-excited biomolecules. *Biophys. J.* 66:430–436.

Mathews, A. J., R. J. Rohlfs, J. S Olson, J. Tame, J.-P. Renaud, and K. Nagai. 1989. The effects of E7 and E11 mutations on the kinetics of ligand binding to R-state human hemoglobin. *J. Biol. Chem.* 264:16573–16583.

Maxwell, J. C., and W. S. Caughey. 1976. An infrared study of NO bonding to heme B and hemoglobin A. Evidence for inositol phosphate induced cleavage of proximal histidine to iron bonds. *Biochemistry.* 15:388–396.

Mourant, J. R., D. P. Braunstein, K. Chu, H. Frauenfelder, G. U. Nienhaus, P. Ormos, and R. D. Young. 1993. Ligand binding to heme proteins. II. Transitions in the heme pocket of myoglobin. *Biophys. J.* 65:1496–1507.

Nagai, K., B. Luisi, K. Shih, G. Miyazaki, K. Imai, C. Poyart, A. DeYoung, L. Kuriatkowsky, R. W. Noble, S.-H. Lin, and N. T. Yu. 1987. Distal residues in the oxygen binding site of haemoglobin studied by protein engineering. *Nature.* 329:858–860.

Nagai, K., T. Kitagawa, and H. Morimoto. 1980. Quaternary structure and low frequency molecular vibrations of haems of deoxy- and oxyhaemoglobin studied by resonance Raman scattering. *J. Mol. Biol.* 136:217–289.

Nienhaus, G. U., J. R. Mourant, and H. Frauenfelder. 1992. Spectroscopic evidence for conformational relaxation in myoglobin. *Proc. Natl. Acad. Sci. USA.* 89:2902–2906.

Nienhaus, G. U., J. R. Mourant, K. Chu, and H. Frauenfelder. 1994. Ligand binding to heme proteins: the effect of light on ligand binding in myoglobin. *Biochemistry.* 33:13413–13430.

Olson, J. S., A. J. Mathews, R. J. Rohlfs, B. A. Springer, K. D. Egeberg, S. G. Sligar, J. Tame, J. P. Renaud, and K. Nagai. 1988. The role of the distal histidine in myoglobin and haemoglobin. *Nature.* 336:265–266.

Park, K. D., K. Guo, F. Adebodun, M. L. Chiu, S. G. Sligar, and E. Oldfield. 1991. Distal and proximal ligand interactions in heme proteins: correlations between C-O and Fe-C vibration frequencies, oxygen-17 and carbon-13 nuclear magnetic resonance chemical shifts, and oxygen-17 nuclear quadrupole coupling constants in $C^{17}O$- and ^{13}CO-labeled species. *Biochemistry.* 30:2333–2347.

Phillips, G. N., Jr., R. M. Arduini, B. A. Springer, and S. G. Sligar. 1990. Crystal structure of myoglobin form a synthetic gene. *Proteins Struct. Funct. Genet.* 7:358–365.

Post, F., W. Doster, G. Karvounis, and M. Settles. 1993. Structural relaxation and nonexponential kinetics of CO-binding to horse myoglobin — multiple flash photolysis experiments. *Biophys. J.* 64:1833–1842.

Powers, L., B. Chance, M. Chance, B. Campbell, J. Friedman, S. Khalid, C. Kumar, A. Naqui, K. S. Reddy, and Y. Zhou. 1987. Kinetic, structural, and spectroscopic identification of geminate states of myoglobin: a ligand binding site on the reaction pathway. *Biochemistry.* 26:4785–4796.

Reddy, N. R. S., P. A. Lyle, and G. J. Small. 1992. Application of spectral hole burning spectroscopies to antenna and reaction center complexes. *Photosynth. Res.* 31:167–194.

Ray, G. B., X. Y. Li, J. A. Ibers, J. L. Sessler, and T. G. Spiro, 1993. How far can proteins bend the FeCO unit — distal polar and steric effects in heme proteins and models. *J. Am. Chem. Soc.* 116:162–176.

Rousseau, D., and J. R. Friedman. 1988. Transient and cryogenic studies of photodissociated hemoglobin and myoglobin. *In* Biological Applications of Raman Spectroscopy. T. G. Spiro, editor. John Wiley & Sons, New York. 133–216.

Sambrook, J., E. F. Fritsch, and T. Maniatis. 1989. Molecular Cloning: A Laboratory Manual. Cold Spring Harbor Laboratory Press, Cold Spring Harbor, NY.

Scheidt, W. R., and D. M. Chipman. 1986. Preferred orientation of imidazole ligands in metalloporphyrins. *J. Am. Chem. Soc.* 108:1163–1167.

Schlichting, I., J. Berendzen, G. N. Phillips, Jr., and R. M. Sweet. 1994. Crystal structure of photolysed carbonmonoxy-myoglobin. *Nature.* 371: 808–812.

Shu, L., and G. J. Small. 1992. Mechanism of nonphotochemical hole burning: cresyl violet in polyvinyl alcohol films. *J. Opt. Soc. Am. B.* 9:724–732.

Smerdon, S. J., S. Krzywda, A. J. Wilkinson, R. E. Brantley, Jr., T. E. Carver, M. S. Hargrove, and J. S. Olson. 1993. $Serine^{92}$ (F7) contributes to the control of heme reactivity and stability in myoglobin. *Biochemistry.* 32:3132–3138.

Springer, B. A., and S. G. Sligar. 1987. High-level expression of sperm whale myoglobin in *Escherichia coli. Proc. Natl. Acad. Sci. USA.* 84: 8961–8965.

Springer, B. A., K. D. Egeberg, S. G. Sligar, R. J. Rohlfs, A. J. Mathews, and J. S. Olson. 1989. Discrimination between oxygen and carbon monoxide and inhibition of autooxidation by myoglobin. Site-directed mutagenesis of the distal histidine. *J. Biol. Chem.* 264:3057–3060.

Srajer, V., L. Reinisch, and P. M. Champion. 1991. Investigation of laser-induced long-lived states of photolyzed MbCO. *Biochemistry.* 30:4886–4895.

Steinbach, P. J., A. Ansari, J. Berendzen, D. Braunstein, K. Chu, B. R. Cowen, D. Ehrenstein, H. Frauenfelder, J. B. Johnson, D. C. Lamb, S. Luck, J. R. Mourant, G. U. Nienhaus, P. Ormos, R. Philipp, A. Xie, and R. D. Young. 1991. Ligand binding to heme proteins: the connection between dynamics and function. *Biochemistry.* 30:3988–4001.

Young, R. D., H. Frauenfelder, J. B. Johnson, D. C. Lamb, G. U. Nienhaus, R. Philipp, and R. Scholl. 1991. Time- and temperature dependence of large-scale conformational transitions in myoglobin. *Chem. Phys.* 158: 315–328.

Zollfrank, J., Friedrich, F., and Parak, F. 1992. Spectral hole-burning study of protoporphyrin IX-substituted myoglobin. *Biophys. J.* 61:716–724.